minerals

MDPI

Article

Coupling Relationships between Sedimentary Microfacies, Sand Bodies, and Tectonic Fracture Characteristics in Braided River Deltas: A Case Study of the Bashijiqike Formation in the Keshen 2 Area

Zhuangsheng Wang [1,2], Xiaobing Lin [1,2,*], Songbai Zhu [3], Junming Fan [1] and Yuchao Zheng [1]

[1] Key Laboratory of Deep-Time Geography and Environment Reconstruction and Applications of Ministry of Natural Resources, Institute of Sedimentary Geology, Chengdu University of Technology, Chengdu 610059, China; 19980830820@163.com (Z.W.); dark_knight_0000@163.com (J.F.); 13008151275@163.com (Y.Z.)
[2] Institute of Sedimentary Geology, Chengdu University of Technology, Chengdu 610059, China
[3] Tarim Oilfield, PetroChina, Korla 841000, China; zsbai-tlm@petrochina.com.cn
* Correspondence: linxiaobing07@cdut.edu.cn

Abstract: Fractures are crucial as main natural gas transport channels in tight sandstone reservoirs. In order to reveal the correlation between the combination of fractures in Block Keshen 2 and sandstone, we have collected drilling core data, logging curve data, imaging logging data, and rock thin-section data from the Bashjiqike Formation in the Keshen 2 area, and by classifying and statistically analyzing the different influencing factors of fractures, we have established a correlation between the development of fractures and sandstone thickness, lithology, and sedimentary microfacies. The results reveal the following: (1) frequent vertical superposition and lateral migration occur in the sedimentary sand bodies of the Bashijiqike Formation. Three types of patterns of sand bodies have been identified according to the changes in microfacies. Type I refers to the patterns of sand bodies developed in main subaqueous distributary channels, type II refers to the patterns of sand bodies developed in secondary subaqueous distributary channels or mouth bars, and type III refers to the patterns of sand bodies developed in isolated subaqueous distributary channels; (2) three types of fracture patterns have been described in the various sand bodies of the Bashijiqike Formation in the Keshen area, including high–medium-angle branch-like fracture patterns, medium-angle reticular fracture patterns, and isolated fractures; (3) the coupling relationship among sedimentary microfacies, sand body patterns, and fracture patterns has been established. The high–medium-angle branch-like fracture patterns mainly develop in the main underwater distributary channel and the type I sand body patterns. The medium-angle reticular fracture patterns mainly develop in the secondary underwater distributary channel and mouth bars, as well as the type II sand body patterns. Isolated fractures can occur in all sedimentary microfacies but are sporadically distributed within the three types of sand body patterns. The research results present the regularity of fracture development in fractured reservoirs, which can be applied to oil and gas fields with the same background, providing certain geological evidence for exploration and development.

Keywords: braided river delta; sedimentary sand body patterns; fracture complex; response model; Bashijiqike formation; Kuqa depression

Citation: Wang, Z.; Lin, X.; Zhu, S.; Fan, J.; Zheng, Y. Coupling Relationships between Sedimentary Microfacies, Sand Bodies, and Tectonic Fracture Characteristics in Braided River Deltas: A Case Study of the Bashijiqike Formation in the Keshen 2 Area. *Minerals* **2023**, *13*, 1020. https://doi.org/10.3390/min13081020

Academic Editor: Stephen E Laubach

Received: 15 June 2023
Revised: 22 July 2023
Accepted: 29 July 2023
Published: 30 July 2023

1. Introduction

Fractures can effectively improve the physical properties of tight sandstone reservoirs and create migration channels for hydrocarbon accumulation [1–3]. Therefore, in recent years, extensive research has focused on the challenging issues related to fracture formation mechanisms and the distribution of tight sandstone reservoirs. Many scientists have conducted research on the relationship between fractures and sand bodies, placing greater

emphasis on the impact of fractures on fluids and the transmission models controlled by fractures [4–6]. The Lower Cretaceous Bashijiqike Formation in the Kelasu structural zone of the Kuqa Depression represents an ultra-deep fractured tight sandstone reservoir with poor matrix physical properties. However, the widespread presence of fractures in the Keshen 2 gas field leads to significant development benefits.

Previous researchers conducted extensive statistical analysis and studies on the developmental stages, filling degree, opening, attitude, influencing factors, and development laws of tectonic fractures in the Bashijiqike Formation in the Kuqa Depression. These studies were based on field fracture outcrop observations, 3D seismic interpretation of fractures, fracture identification using image logs, and microscopic thin-section observations. As a result, multiple fracture prediction methods have been proposed, including the two-factor method [7–9], the curvature method [10–13], the fractal geometry and fractal dimension methods [14–16], and the seismic attribute method [17–19]. The development of tectonic fractures is primarily influenced by factors such as lithology, strata depth, rock layer thickness, tectonic parts, and tectonic stress. However, these factors can have different or opposite effects on tectonic fractures under various tectonic settings and sedimentary environments [20]. Consequently, using different individual factors and prediction methods leads to significantly different predicted results. Furthermore, the composite prediction using multiple factors is challenging due to the contradictions among parameters, and simple numerical simulations fail to reflect the cognitive laws of complex geological conditions. The same influencing factor can also affect fractures in oil and gas reservoirs with distinct structural conditions. Therefore, applying fracture prediction methods widely is often difficult, and some researchers argue that it is only practical to predict individual oil and gas reservoirs [21–23].

Sedimentary facies are composed of sedimentary material composition and sedimentary environment; therefore, different sedimentary facies have different characteristics such as rock composition, lithological combination, and rock distribution range and thickness. For the study area, braided river delta sedimentary facies can be identified. There are many types of deltas, each with different characteristics. For other different types of deltas, the grain size of sedimentary materials in braided river delta facies is finer, the transport distance is farther, and the differentiation characteristics of gravity sedimentation are obvious [24,25]. Previous studies have shown an inverse correlation between tectonic fractures in the Keshen 2 gas field and stratum depth, as well as an inverse proportionality with rock layer thickness [2]. Uniaxial compressive strength tests indicate that the compressive strength of sandstones with different components follows the order of pure sandstones > sandstones with a large number of mudstones > sandstones with a small number of mudstones [26]. Moreover, splitting tensile strength tests (Brazilian) reveal the failure modes of mudstones. Pure sandstones primarily undergo longitudinal shear failure with penetrability, whereas sandstones with argillaceous components mainly experience longitudinal splitting, with the argillaceous content being inversely correlated with the splitting angle [26]. In the Keshen 2 gas field, which has a consistent burial depth, the rock composition, lithologic associations, and rock layer thickness and heterogeneity are primarily controlled by the paleo-depositional environment.

To gain further insights, this study conducted a comprehensive analysis using core observations, thin-section analyses, rock and mineral experiments, image logs, and inter-well remote detection of the Keshen 2 gas field in the Kuqa Depression. Based on these extensive data, the study determined the superimposition and patterns types of sedimentary sand bodies and summarized the developmental patterns of fractures through a detailed characterization of sedimentary microfacies. Finally, a response model of sedimentary microfacies–sedimentary sand bodies fracture characteristics was established under the same tectonic setting. This study offers a new perspective for accurately predicting fractures while considering the constraints imposed by sedimentary microfacies.

2. Geological Setting

The Kuqa Depression, located in the northern part of the Tarim Basin, underwent various geological transformations throughout different periods. It originated as a foreland basin during the Late Permian to the Triassic period and later changed into a faulted basin and depression during the Jurassic era. Eventually, it evolved into a resurgent foreland basin from the Cretaceous to the Quaternary period. These geological processes formed eight secondary structural units, including four structural zones, three depression zones, and one uplift zone [27]. The Keshen area in the Kelasu structural zone is influenced by a series of thrusting faults oriented in an east–west direction. These faults have led to the creation of multiple faulted anticline traps. Recent exploration efforts have uncovered numerous large- and medium-sized oil and gas reservoirs in this region [28] (Figure 1a,b).

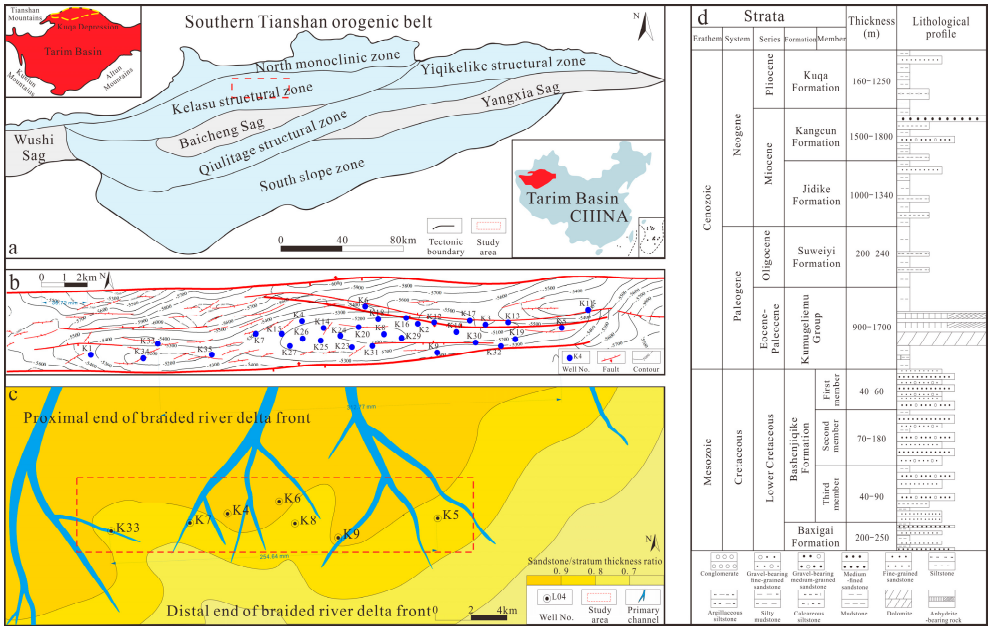

Figure 1. Structural location and stratigraphic development characteristics of the study area. (**a**) Structural location map of the Kuqa Depression (according to [27] revised). (**b**) Well location map of the research area (provided by Kela Oil and Gas Production Management Zone of PetroChina Tarim Oilfield Branch). (**c**) Revised location of the research area (according to [28] revised). (**d**) Comprehensive stratigraphic column of the study area (according to [29] revised).

Drilling activities in the Keshen area have encountered various strata, including the Quaternary (Q), Neogene Kuqa (N_2k), Kangcun ($N_{1\text{-}2}k$), and Jidike (N_1j) formations, the Paleogene Suweiyi Formation ($E_{2\text{-}3}s$) and Kumugeliemu Group ($E_{1\text{-}2}km$), and the Cretaceous Bashenjiqike (K_1bs) and Baxigai (K1bx) formations from top to bottom, although some wells never penetrated across the Bashenjiqike and Baxigai formations [29]. During the Cretaceous period, characterized by a dry climate, the southern Tianshan Mountains experienced uplift, providing ample source material. As water bodies flowed out of the mountain pass and entered the gentle basin areas, they significantly slowed down, leading to the rapid and widespread deposition of transported materials. Consequently, the Keshen area formed widely distributed, thick sand bodies of the braided river delta front subfacies [27]. These sand bodies exhibit a high sandstone/stratum thickness ratio, ranging from 80% to 98%. The Keshen 2 gas field measures approximately 3 km in width from north to south and around 27 km in length from east to west. The dominant sedimentary microfacies in the gas field include subaqueous distributary channels, mouth bars, and interdistributary bays at the proximal end of the braided river delta front (Figure 1c).

The main gas reservoir in the Keshen 2 gas field comprises thick, tight sandstones from the Cretaceous Bashijiqike Formation (Figure 1d). These sandstones are 200–300 m

in thickness and are buried at depths ranging from 6000–7000 m. They exhibit a matrix porosity of 1.5%–5.5% and a matrix permeability of (0.01–0.10) $\times$ 10^{-3} μm^2. This reservoir is characterized by fractures, classifying it as an ultra-deep fractured tight sandstone type [30–32].

3. Materials and Methods

We obtained 27 sets of drilling data from the Keshen area (see Figure 1b for well locations), including drilling lithology records (a total of 27 well drilling core records with a total length of 5230 m), logging curve data (a total of 5813.1 m logging data for 27 wells with data point intervals of 0.125 m), acoustic imaging logging data (a total of 2136.2 m for 13 wells), electrical imaging logging data (a total of 1013.8 m for 8 wells), core thin-sections (a total of 65 pieces), and core observation data (a total of 153 m core section for 7 wells). All data are provided by the Kela Oil and Gas Production Management Area of PetroChina Tarim Oilfield Branch.

3.1. Core Data

The core data include drilling core data (core photos and core observation records) and core thin-section data. These data are collected from the core storage within the permitted scope of CNPC Tarim Oilfield Branch. The core photos were taken on-site at the core library of CNPC Tarim Oilfield Branch, using Canon (w) DSLR cameras. The core thin-sections were sampled and produced under the permission of CNPC Tarim Oilfield Branch with a sampling interval of 1 m. The SYJ-200 fully automatic precision cutting machine was used for longitudinal core cutting, and the samples were ground using the UNIPOL-1202 fully automatic precision grinding machine. The ground samples were then polished using the GPC-80A precision grinding and polishing control instrument. The resin-filling and glass-covering operations were completed using the MTI-3040 heating table and DZF-6020 vacuum drying oven. Rock thin-section identification and scanning electron microscopy analysis was performed at the Institute of Sedimentary Geology, Chengdu University of Technology, per the Technical Specification for Rock and Mineral Identification in the Geological and Mineral Industry Standards of the People's Republic of China DZ/T0275.1-2015. Rock thin-section identification used an optical microscope (Nikon E600 POL, Tokyo, Japan), and SEM used an scanning electron microscope (S4800), The highest resolution is 1.4 nm, with a magnification of 20×–800,000×.

3.2. Logging Data

The logging data comprise logging curve data and imaging logging result data (including acoustic imaging logging and electrical imaging logging) provided by the logging database of the CNPC Tarim Oilfield Branch. The logging data underwent depth correction based on the core section of the Bashijiqike Formation. A total of 5813.1 m of lithology logging correction was completed for 27 wells, including gamma ray (GR), KTH, M2R3, M2R6, and M2RX logging curves. The interpretation point intervals were set at 0.125 m. The logging curve data were processed using Res-From GeoOffice v3.5 software developed by Kaben Company. Outliers were removed by correcting the depth of the logging curve. The imaging logging data were sourced from the logging database of the PetroChina Tarim Oilfield Branch in 2019 and were based on the interpretation results of Baker Hughes Company in 2013 and Schlumberger Company in 2014. The recognition results are displayed in FMI images and OBMI image results. The FMI and OBMI images were identified and interpreted by the Logging Center of the Exploration and Development Research Institute of the Tarim Oilfield Branch of China National Petroleum Corporation. A total of 21 wells underwent imaging logging interpretation and identification work, resulting in a total of 3150 m. The interpretation results of imaging logging data effectively identified bedding planes, high conductivity fractures, and high resistance fractures. Additionally, they provided data on fracture inclination, dip angle, and penetration length.

3.3. Research Methods

3.3.1. Analysis Methods of Sedimentary Facies and Sand Bodies

Based on the core data, the lithologic association, mineral composition, sedimentary structure, lithologic inter-face, and other characteristics of the Bashijiqike Formation in the Keshen 2 area were identified. At the same time, using rock thin-section data to analyze its main clastic and interstitial components, determine its sedimentary environment, and use logging curves to assist in completing sedimentary phase change analysis, the sedimentary facies type and sedimentary sand body combination type were determined. It mainly develops braided river delta sedimentary facies in the river–lake transition zone, primarily composed of underwater distributary channel microfacies, estuarine dam microfacies, and interdistributary bay microfacies. Based on the corrected logging curve data, three types of sedimentary sand body combinations were comprehensively identified, representing different sedimentary environments.

3.3.2. Statistics of Fractures

Fracture statistics are mainly conducted through the interpretation results of electrical imaging logging and acoustic imaging logging provided by PetroChina Tarim Oilfield Company. These interpretation results will identify the bedding planes, joint planes, and fractures identified by imaging logging, and we will select the fracture data for processing. We extracted the data displayed in the interpretation results, such as the number of fractures, fracture penetration length, and fracture dip angle, and combined the development of fractures into different types of fracture combinations based on the occurrence of centrally developed fractures.

3.3.3. Coupling Relationship

The coupling relationship between sedimentary sand body and fracture development is determined by comparing the development of different sedimentary sand body types with the imaging logging interpretation of fractures and considering characteristics such as fracture inclination, dip angle, and penetration length. A response model for developing sedimentary microfacies sand body combination fractures is established.

4. Results

4.1. Characteristics of Sedimentary Microfacies and Sand Body Patterns

4.1.1. Characteristics of Sedimentary Microfacies

Many previous studies have been conducted on the sedimentary microfacies in the Keshen area, and it is generally believed that the Keshen 2 area has a sedimentary environment similar to that of the braided river delta front sub-facies. This area has developed microfacies such as subaqueous distributary channels, mouth bars, and interdistributary bays. This study builds upon previous research and incorporates data from cores, thin-section identification, and scanning electron microscopy to further identify the main and secondary subaqueous distributary channel microfacies (Figure 2). These microfacies exhibit the following characteristics.

Main subaqueous distributary channel microfacies: a main subaqueous distributary channel is the sub-aqueous extension part of a braided channel. Compared to a secondary channel, the sedimentary sand bodies in a main channel have larger grain sizes and greater thicknesses. The lithology of the main channel mainly consists of fine-grained sandstones. Typical parallel bedding has developed (Figure 2a–c).

Secondary subaqueous distributary channel microfacies: unlike a main channel, a secondary channel exhibits weaker hydrodynamic forces. Consequently, the sedimentary sand bodies in a secondary channel have smaller grain sizes and lesser thicknesses. The lithology of a secondary channel comprises fine-grained sandstones and siltstones. A secondary channel tends to be superimposed with the mouth bar microfacies (Figure 2d–f).

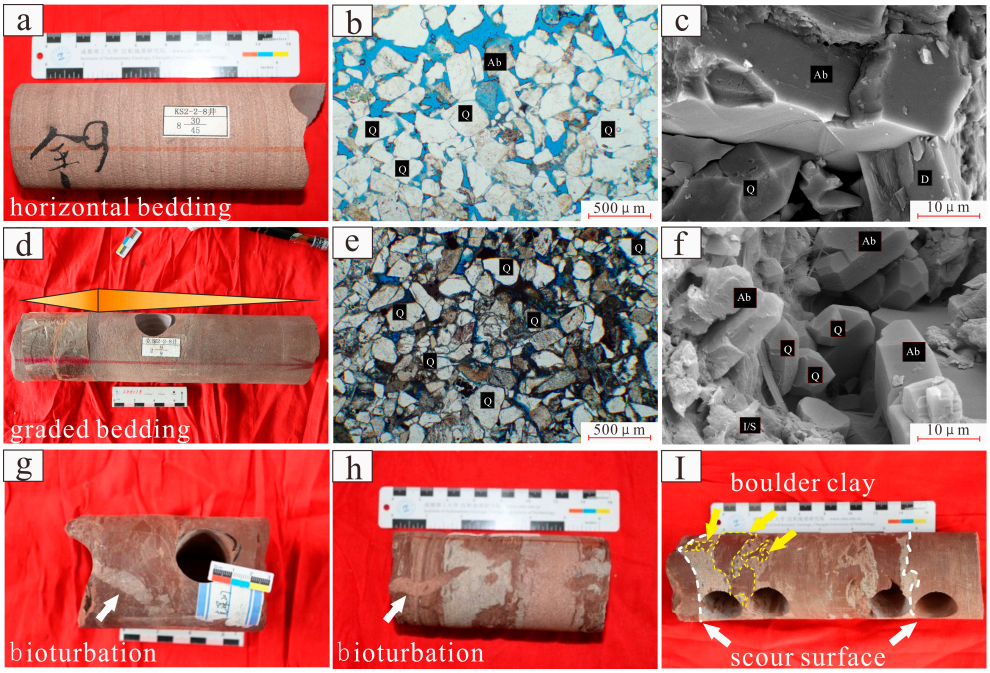

Figure 2. Characteristics of the identification indicators of sedimentary microfacies. (**a**). Well K31, depth: 6818 m, fine-grained sandstones, with parallel bedding developing; (**b**). Well K31, depth: 6178.2 m, medium- and fine-grained lithic feldspar sandstones, with visible intergranular pores and intergranular corroded residual pores; (**c**). Well K24, depth: 6560.92 m, quartz, orthoclase particles; (**d**). Well K31, depth: 6716.5 m, siltstones, indicating microfacies of mouth bars and secondary subaqueous distributary channels; (**e**). Well K31, depth: 6199.5 m, fine-grained lithic feldspar sandstones, with intergranular pores visible; (**f**). Well K31, depth: 6199.5 m, quartz, feldspar grains, with mixed-layer illite–smectite as fillings; (**g**). Well K9, depth: 6875.6 m, mudstones, indicating interdistributary bay microfacies; (**h**). Well K31, depth: 6714.5 m, mudstones, indicating interdistributary bay microfacies; (**I**). Well K3, depth: 6709.3 m, mudstones, erosion surface, indicating interdistributary bay microfacies.

4.1.2. Classification and Characteristics of Sand Body Types

The Cretaceous Bashijiqike Formation in the Keshen area exhibits frequent vertical superimposition and horizontal migration of sedimentary microfacies. Consequently, the sedimentary sand bodies formed in this depositional environment have diverse and complex superimpositions and combinations. An analysis of 27 drilling data drilled in the Keshen area reveals that the sand bodies in the Bashijiqike Formation are primarily deposited in subaqueous distributary channels and mouth bars, forming three distinct patterns types (Table 1, Figure 3).

A type I sand body patterns refers to the collection of thick sand bodies within a main subaqueous distributary channel (Figure 3).

Type I sand body patterns mainly develop within the subaqueous distributary channel microfacies and result from the long-term deposition of main channels. These single-layer sand bodies have a small thickness, typically 10 to 20 m, and exhibit well-preserved normally rhythmic cycles. After undergoing scouring and elutriation under strong hydrodynamic forces, the sandstones within type I sand body patterns are pure and contain a small number of argillaceous materials. They predominantly consist of fine to medium-grained sandstones. The GR and R curves of type I sand body patterns are primarily box-shaped or exhibit a box with saw teeth.

A type II sand body pattern is formed by superimposing multiple sets of sand bodies within subaqueous distributary channels and mouth bars (Figure 3).

Type II sand body patterns mainly develop within the subaqueous distributary channel microfacies and mouth bar microfacies. They are created by superimposing sand bodies

from various microfacies under a sedimentary environment that frequently changes due to channel migration and lake-level fluctuations. The single-layer sandstones within type II sand body patterns have a small thickness, generally ranging from 1 to 2 m, while their total thickness typically ranges from 5 to 25 m. Although their preservation is incomplete, these patterns exhibit repeated superimposition of normally and reversely rhythmic cycles. Due to significant changes in hydro-dynamic forces, the sedimentary sand bodies undergo long-term migration and erosion. Consequently, they contain significant residual argillaceous materials and often feature thin layers with boulder clay. The predominant lithologies are fine-grained sandstones, siltstones, argillaceous siltstones, and boulder clay-bearing siltstones. The shapes of the GR curves within type II sand body patterns are characterized by the superposition of boxes with saw teeth and bells with saw teeth.

A type III sand body patterns refers to the collection of sand bodies within isolated subaqueous distributary channels (Figure 3).

Type III sand body patterns form through the single-stage deposition of secondary subaqueous distributary channels. The single-layer sand bodies within type III patterns have a small thickness, ranging from 2 to 5 m, and are separated by mud–stone interlayers. The lithology primarily consists of fine-grained sandstones and medium–fine-grained sandstones. The GR curves of type III sand body patterns are wide finger-shaped.

Table 1. Sand body patterns types in the Bashijiqike Formation in the Keshen 2 gas field.

Sand Body Patterns Type	Sedimentary Microfacies	Sedimentary Environment	Total Thickness (m)	Single-Layer Thickness (m)	Main Lithology	(K/mD, Φ/%)	Logging Curves (GR, R)	Reservoir Space
Type I	Main subaqueous distributary channel microfacies	Main subaqueous distributary channels	10–20	5–10	Fine-grained sandstones	0.03–0.12 4–12	Box-shaped curves that are relatively smooth and flat or have low-amplitude saw-teeth	Intergranular pores, with high connectivity of pore throats
Type II	Secondary subaqueous distributary channel microfacies and mouth bar microfacies	Secondary subaqueous distributary channels and mouth bars	5–25	1–2	Argillaceous siltstones, siltstones, and fine-grained sandstones	0.01–0.1 4–9	Box-, bell-, or funnel-shaped curves with saw-teeth	Intergranular pores and micropores, with medium connectivity of pore throats
Type III	Subaqueous distributary channel microfacies	Isolated subaqueous distributary channels	2–5	2–5	Siltstones, and fine-grained sandstones	0.01–0.08 1–6	Wide exponent-shaped curves	Intergranular pores and micropores, with poor connectivity of pore throats

4.2. Patterns of Fracture Patterns Development

Based on the characteristics of fractures in different types of sedimentary sand body patterns in the Keshen area, this study summarizes three coupling patterns of sand body patterns with fractures, namely, high–medium-angle branch-like fracture patterns, medium-angle reticular fracture patterns, and isolated fractures (Figure 4).

(1) High–medium-angle branch-like fracture patterns: in this pattern, a small number of vertical fractures with nearly vertical angles, long extension distances, large openings, and low filling degrees, along with a large number of fractures with medium–high angles, form fracture complexes where the two types of fractures connect. This type of fracture patterns mostly occurs in type I sand body patterns;

(2) Medium-angle reticular fracture patterns: in this pattern, medium-angle reticular fractures of different attitudes form complex reticular fracture patterns mostly developed in type II sand body patterns. The medium-angle reticular fractures in this pattern have short fracture extensions, small openings, and high filling degrees;

(3) Isolated fractures: isolated fractures mainly develop near the contact surface between sandstones and mudstones. They are generally medium-angle fractures with a small number and scale. Isolated fractures generally occur in type III sand body patterns.

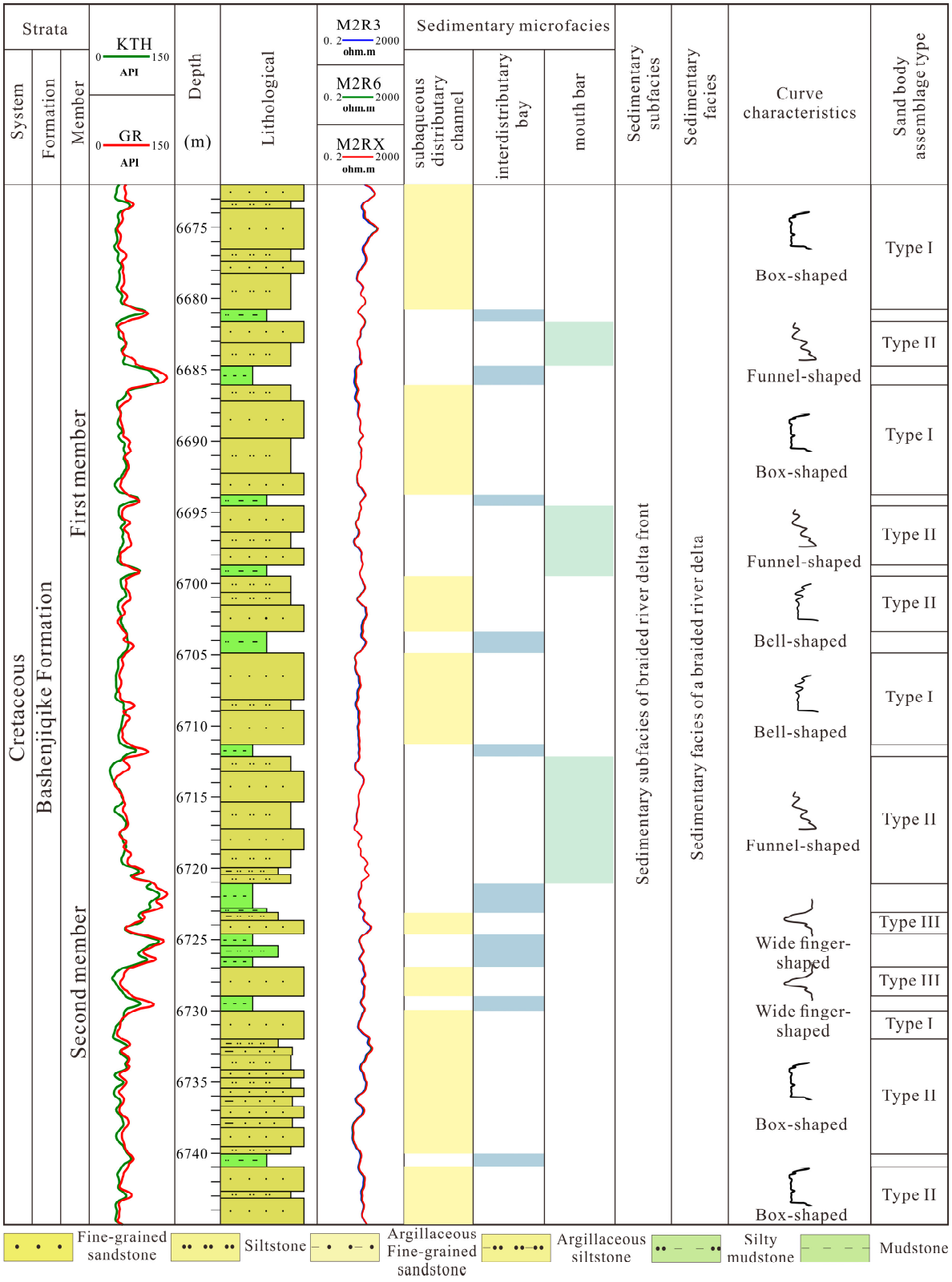

Figure 3. Sedimentary microfacies and sand body types (e.g., the well K26).

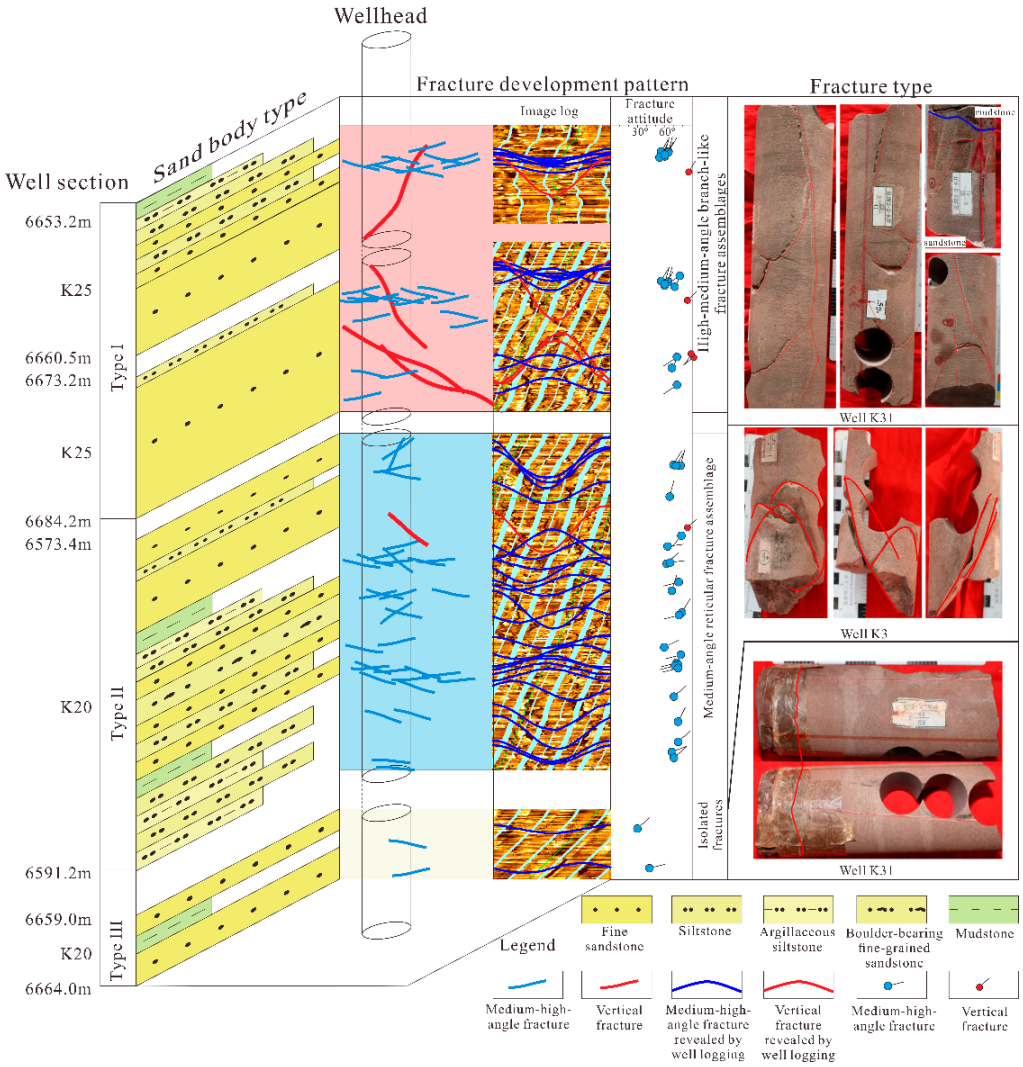

Figure 4. Coupling patterns of sand bodies with fracture patterns.

5. Discussion

5.1. Influencing Factors in Fracture Development

5.1.1. Tectonic Locations

The tectonic factor predominates among the influencing factors in fracture development. Rocks within strata are subjected to varying tectonic stresses in different tectonic locations, resulting in significant disparities in the types, extent of opening, and degree of filling of fractures [2].

The Keshen 2 block is situated within a series of thrust-shingled structures in the overall Kelasu tectonic zone. The gas reservoir within this block maintains a consistent burial depth and is characterized as a thrust anticline as a whole [33–35]. This anticline follows a north–south trend, with the north and south wings exhibiting steep dips and the east and west wings displaying gentle dips (Figure 1b). Notably, even within the same structural part, the tectonic fractures show considerable variation (Figure 5). The deposition environment and sediment characteristics are controlled by sedimentary facies, directly influencing factors such as lithology, rock composition, and thickness of rock layers. Consequently, this study examines the influence of different sand body patterns within various sedimentary microfacies on fracture development. The study further investigates the interconnections between sedimentary microfacies, sedimentary sand bodies, and fracture development.

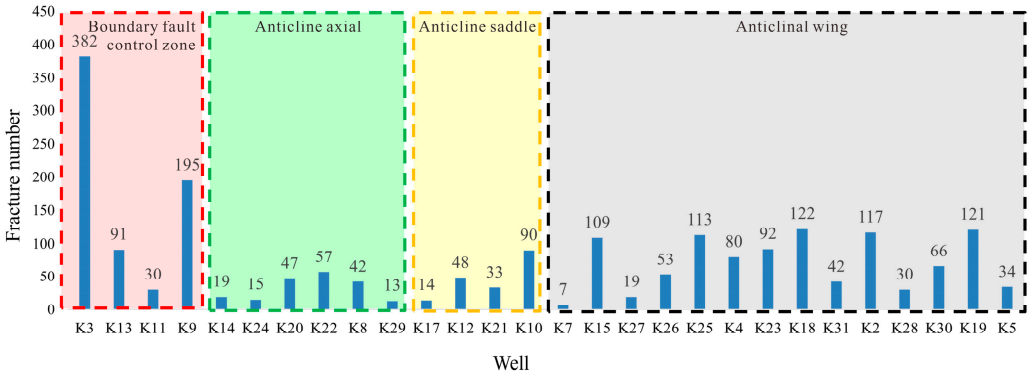

Figure 5. Statistical histogram of cracks in different structural parts of Keshen 2 gas field.

5.1.2. Rock Composition

Fractures are formed when rocks in strata are subjected to stress and sustain damage. The mechanical properties of rocks are influenced by their constituent components, making lithology a crucial intrinsic factor that impacts fracture development.

The proportions of brittle and plastic components in various lithologic compositions significantly affect the mechanical properties of rocks. The degree of fracture development in rocks with different lithologic components follows a specific order: sandstones with argillaceous content of 15%–25% > sandstones with argillaceous content of 25%–50% > sandstones [26]. In addition, mudstones exhibit plastic behavior and tend to undergo plastic deformation when stressed. Consequently, they are less prone to fracturing. As a result, fractures are generally uncommon in mudstones. In the Keshen 2 area, fractures are primarily concentrated in fine-grained sandstones and siltstones (Figure 6). The lithology and rock composition are controlled by the depositional environment and provenance, leading to variations in different sedimentary microfacies.

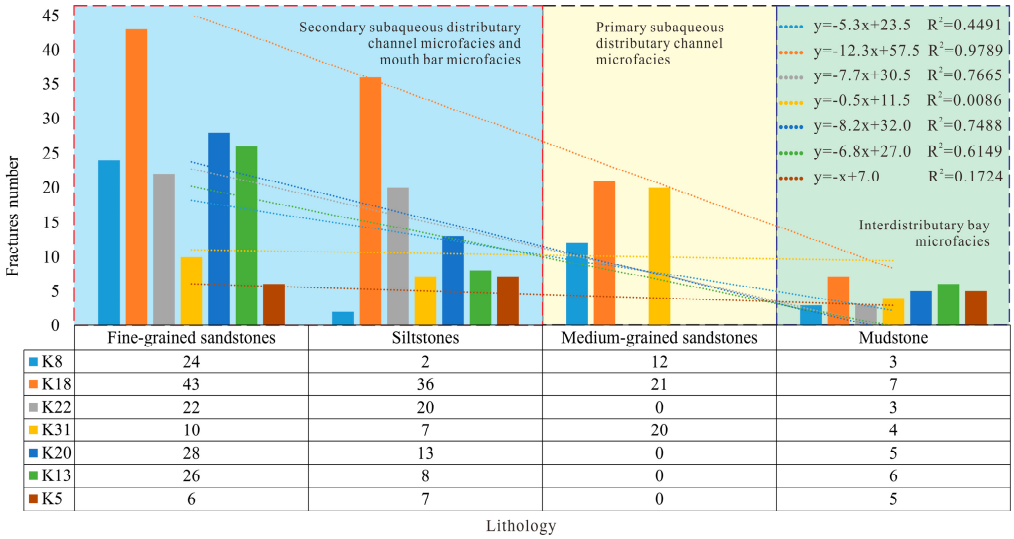

	Fine-grained sandstones	Siltstones	Medium-grained sandstones	Mudstone
K8	24	2	12	3
K18	43	36	21	7
K22	22	20	0	3
K31	10	7	20	4
K20	28	13	0	5
K13	26	8	0	6
K5	6	7	0	5

Figure 6. Statistical histogram of fractures vs. lithology.

Different rock types occur in different sedimentary microfacies. The fine sandstone is mainly deposited in the microfacies of underwater distributary channels, and the sedimentary area is located within the main channel range of underwater distributary channels. Siltstone is mainly developed in the secondary channel and estuary dam of underwater distributary channel. Mudstone mainly exists in the interdistributary bay microfacies.

5.1.3. Sand Body Thickness

The thickness of the rock layers also affects fracture development. As the thickness of the rock layers increases, stress-induced fractured points in the rock layers become increasingly scattered and, as a result, are less likely to interconnect and form fractures. This leads to a lower fracture density. However, thin sandstone strata are more susceptible to breaking under stress. Additionally, the contact surfaces between sandstones and mudstones are weak against stress, making them prone to stress concentration and fracture formation [19]. Fractures are more likely to develop in thin laminated sandstones in the Keshen 2 area (Figure 7). The thickness of the rock layers is determined by the provenance and accommodation in the sedimentary environment and, therefore, varies in different sedimentary environments.

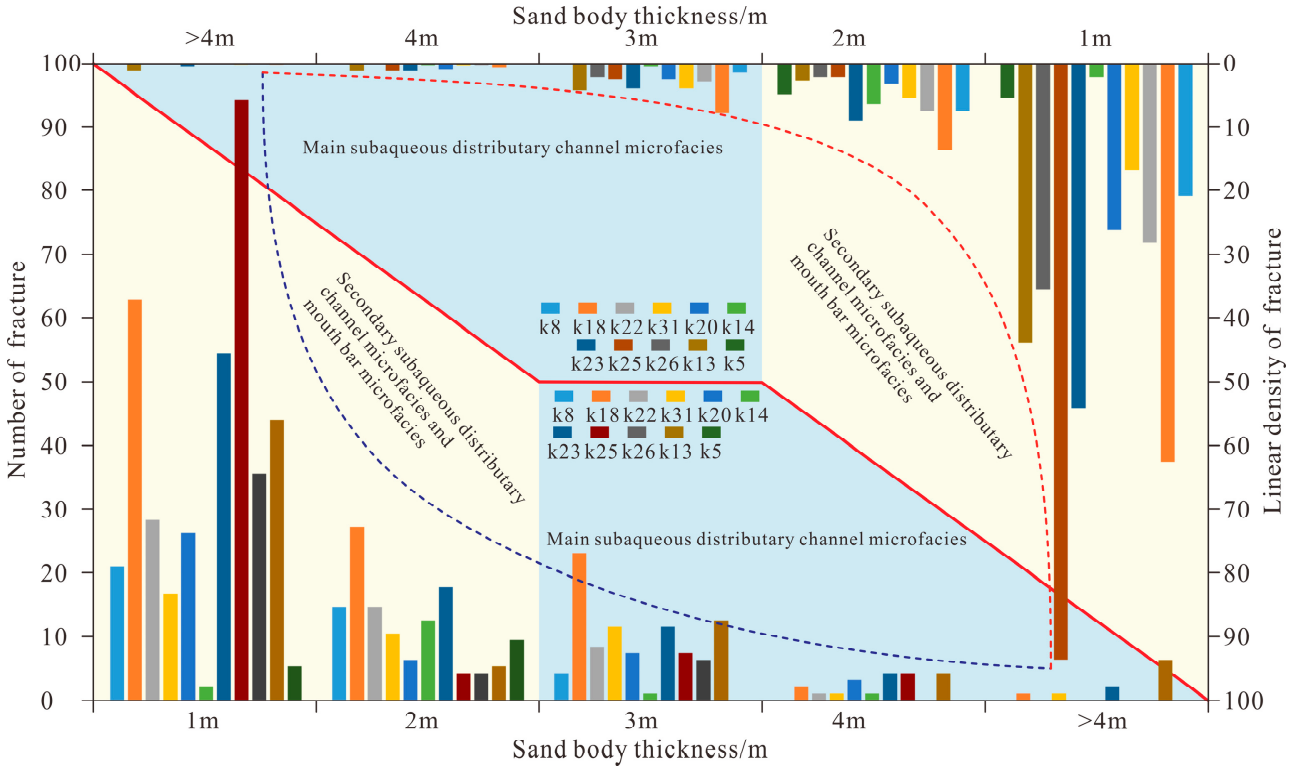

Figure 7. Statistical histogram of fractures vs. sand body thicknesses.

5.1.4. Sedimentary Microfacies

The sedimentary microfacies identified in the Keshen 2 area include main subaqueous distributary channels, secondary subaqueous distributary channels, mouth bars, and interdistributary bays [36,37].

The single-factor statistical analysis (Figure 8) reveals that fractures are mostly developed in secondary subaqueous distributary channels, where medium-angle reticular fractures mainly develop. Fractures are moderately developed in main subaqueous distributary channels, while high–medium-angle branch-like fractures are primarily developed. Fractures are the least developed in mouth bars, with only a few medium-angle reticular fractures.

Overall, constraints on fracture development under the same tectonic setting include differences in influencing factors such as sedimentary microfacies-induced variations in lithologic patterns and rock layer thickness.

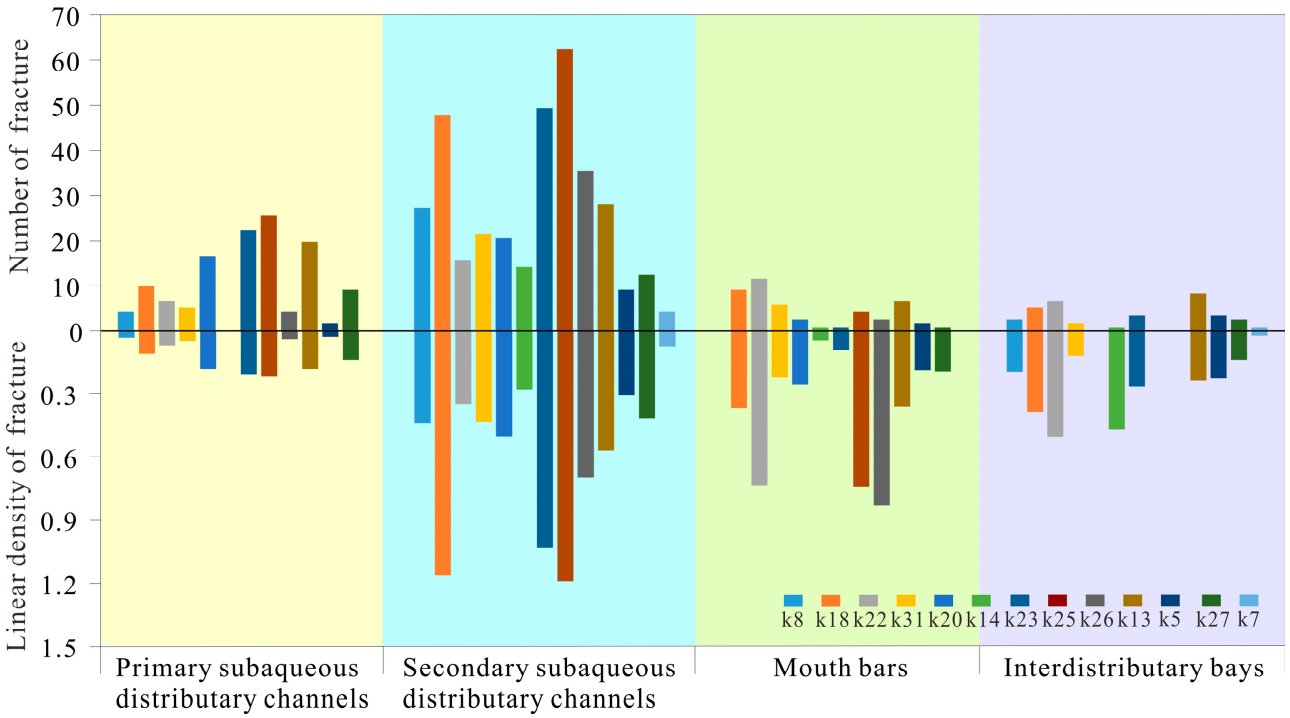

Figure 8. Statistical histogram of fractures vs. sedimentary microfacies.

5.2. Validity of the Coupling Patterns of Sedimentary Sand Bodies with Fracture Development

Based on the coupling patterns of sedimentary sand bodies with fracture patterns development, this study determined the sand body types and fracture development types of every single well in the study area. The well profile shows that the three coupling patterns of sedimentary sand bodies with fracture patterns development proposed in this study closely correlate with the actual logging interpretation of fractures. Specifically, there is a positive correlation between the proportion of sedimentary sand body types and the proportion of fracture development types, and a larger fracture number corresponds to a higher correlation. This finding indicates that the coupling patterns of sedimentary sand bodies with fracture development are consistent with the actual fracture development and can, thus, guide research on the laws and prediction of fracture development (Figure 9).

The type I sand body patterns are mainly deposited in underwater distributary channels, the sand body is thick, and the lithology is mainly siltstone. The overall compressive strength is high, with fewer weak surfaces, requiring greater stress and strain accumulation to cause fractures to occur [38,39]. Type II sand body combinations are developed in the secondary channel of underwater distributary channels or estuary bar sedimentary microfacies, and the developed lithology is mainly siltstone, and the higher mud content compared to the type I sand body combination results in a decrease in the compressive strength of the type II sand body combination. At the same time, the secondary river channel is small in scale and the developed sand bodies are thin, and this also increases the probability of crack development [39]. The combination of type III sand bodies have the highest mud content, and the sand bodies are usually surrounded by mudstone, and mudstone undergoes plastic deformation under pressure and is less prone to cracking, Therefore, the number of isolated fractures usually developing is relatively small [39–42].

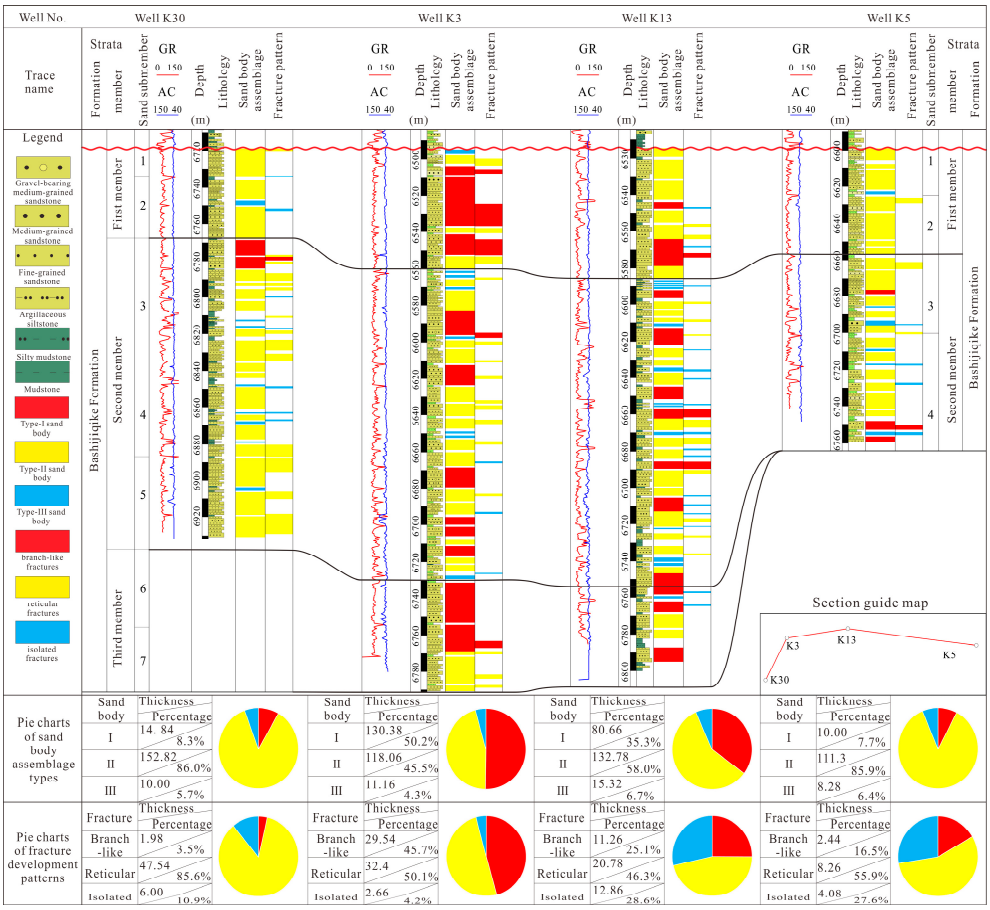

Figure 9. Well profile of fracture patterns.

5.3. Coupling Relationships between Fracture Development and Sedimentary Microfacies

The study area features braided river delta front sub-facies, where various microfacies develop, including subaqueous distributary channels, mouth bars, and interdistributary bays. This study analyzed and classified the sedimentary microfacies of each well, resulting in the creation of sedimentary microfacies plans for the first and second members of the Bashijiqike Formation in the study area. However, the third member of the Bashijiqike Formation was not discovered during the drilling of multiple wells, so there is insufficient fracture interpretation data for this member from the image log [42,43]. Consequently, the first and second members of the Bashijiqike Formation were used in this study to overlay maps displaying fracture development ranges at different horizons onto the sedimentary microfacies plan (Figure 10).

Fracture patterns characterized by high to medium angles resemble branching patterns. These fractures mainly occur within the main subaqueous distributary channel microfacies and are distributed along the extension direction of main channels. Their development is influenced and controlled by the distribution of thick laminated sand bodies within these channels.

Due to the intense hydrodynamic forces in the main subaqueous distributary channel microfacies, unstable components, impurities, and fillings are carried away by water currents during prolonged scouring. The rocks found in the main subaqueous distributary channels primarily consist of quartz sandstones, which exhibit high maturity, a high content of brittle components, and a low argillaceous content. As a result, these rocks are susceptible to longitudinal penetrating shear failure when subjected to tectonic stress, forming high-angle fractures. However, the thick sand bodies within the main subaqueous distributary channel microfacies and the scattered distribution of stress-induced failure points make it challenging for fractures to form. Consequently, only a limited number of fractures develop. Additionally, medium- to low-angle fractures are likely to form along weak surfaces at

the contact interface between sandstones and mudstones [43–45]. The high-angle and medium-angle fractures are inter-connected, creating branch-like fracture patterns.

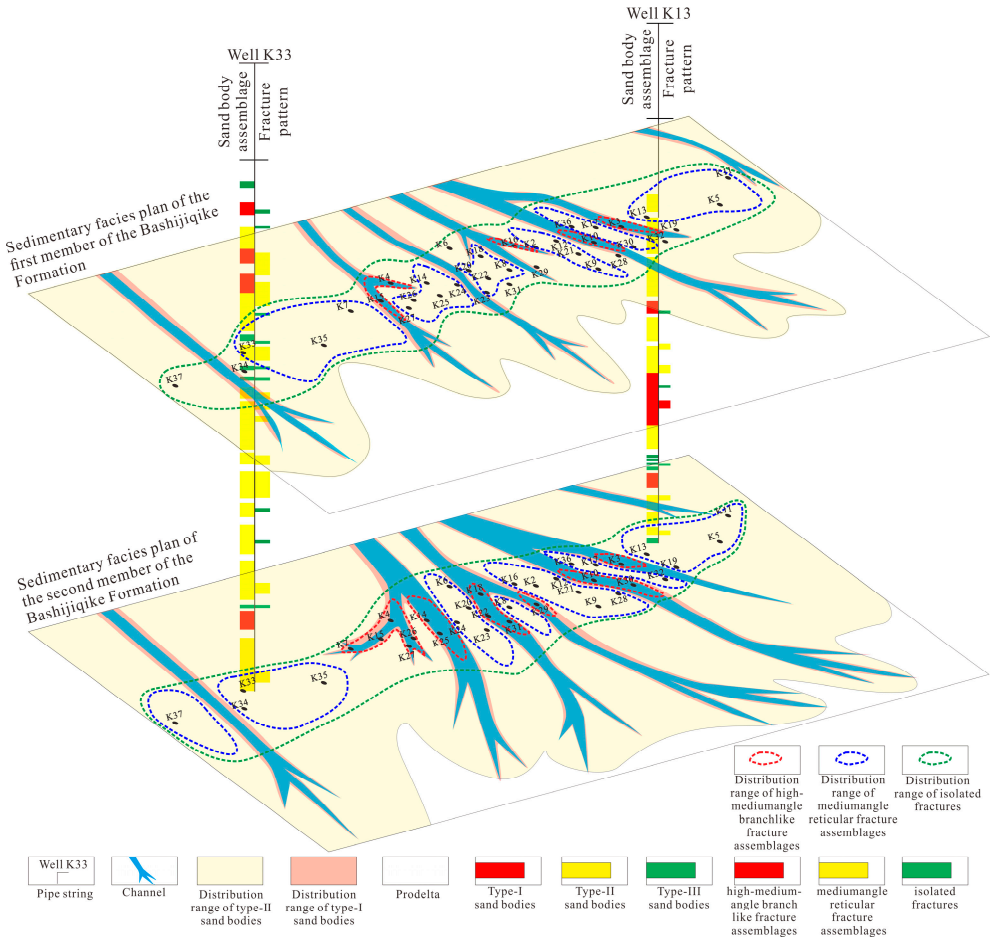

Figure 10. Response model of sedimentary microfacies and fracture development.

Medium-angle reticular fracture patterns are primarily found in secondary subaqueous distributary channel microfacies and mouth bar microfacies. These fractures are distributed along the extension of inter-channel sand bodies on a horizontal plane and are frequently observed in areas with frequent channel migration and superposition. Compared to the other two types of fracture patterns, they are the most developed.

The secondary subaqueous distributary channel microfacies and mouth bar microfacies are characterized by weak hydrodynamic forces. Consequently, secondary channels are prone to frequent migration and lateral aggradation due to wave action in rivers and lakes. Meanwhile, mouth bars exhibit undulation with the lake level and undergo progradation and retrogradation at different stages under the influence of hydrodynamic forces. As a result, the sand bodies deposited in these microfacies are characterized by small scales, small thicknesses, and large quantities. They can be superimposed to form thick laminated sand bodies. With a high clay content, these sand bodies have low compressive strength, making them susceptible to fracturing under tectonic stress. Furthermore, the clay content is inversely proportional to the fracture angle [19], leading to the frequent development of medium-angle fractures. These fractures have a high density and tend to form medium-angle reticular fracture patterns.

Isolated fractures predominantly occur in single-stage subaqueous distributary channel microfacies. They are associated with the interfaces between sandstones and mudstones. Additionally, they are influenced by the fluids retained in the upper and lower mudstones, resulting in high filling degrees.

In general, the development of fractures in the Keshen 2 block is influenced and controlled by different sedimentary microfacies. Therefore, there is a strong correlation between the extent of fracture development and the distribution of sedimentary microfacies. Consequently, under the same tectonic setting, the dominance of sedimentary microfacies in fracture development is pronounced and reflects the actual fracture development. This concept represents a new perspective for understanding the law of fracture development in tight sandstone reservoirs. The interplay between sedimentary microfacies, sand body patterns, and fracture development can be widely applied to predict fractures in tight sandstone reservoirs under the same tectonic setting, guiding the exploration and development of oil and gas reservoirs.

6. Conclusions

The paper presents the development of fractures in ultra-deep sandstone reservoirs in the Keshen 2 area, and reveals three commonly developed sand body patterns types. Establishing the correlation between crack patterns and sand body patterns, the results present a very clear correlation between the combination of fractures and sand bodies. We obtain the following conclusions:

(1) The sedimentary sand body patterns in the Keshen 2 block can be categorized into types I, II, and III based on microfacies. Type I comprises thick laminated sand bodies deposited in main subaqueous distributary channels. Type II consists of patterns formed by the superimposition of sand bodies in secondary subaqueous distributary channels and mouth bars. Type III represents sand bodies occurring in isolated subaqueous distributary channels;

(2) This study identifies three types of correlation between sedimentary microfacies, sand body patterns, and fault complexes in braided river delta.

1. The correlation between high–medium-angle branch-like fracture patterns and type-I sand body patterns is the highest, and type I sand body patterns can only be identified in underwater distributary channel microfacies. The high–medium-angle branch-like fracture patterns complexes consist of a small number of nearly vertical fractures with long extension distances, large openings, and low filling degrees, along with many medium–high-angle fractures interconnecting with each other;
2. The correlation between medium-angle reticular fracture patterns and type II sand body patterns is the highest, and type II sand body patterns can only be identified in underwater distributary channel microfacies and mouth bar microfacies. The medium-angle reticular fracture patterns complex reticular fracture patterns are formed by medium-angle fractures of different orientations intersecting and cutting each other;
3. The correlation between isolated fractures and type III sand body patterns is relatively high, and type III sand body patterns can only be identified in isolated subaqueous distributary channels. The isolated fractures are commonly found near the contact surfaces between sandstones and mudstones, typically exhibiting medium angles, short extension distances, small openings, and high filling degrees.

In summary, the findings of this study provide significant insights into the coupling relationships between sedimentary microfacies, sand body combinations, and fault complexes within Keshen 2 block, situated at the forefront of a braided river delta. It is expected to offer robust geological evidence for oil and gas exploration and development within the block, while also laying the foundation for the study of ultra-deep, fractured, and tight sandstone reservoirs. This research holds great promise for contributing to the sustainable development and utilization of resources in the energy sector.

Author Contributions: Conceptualization, X.L. and Z.W.; methodology, X.L. and Z.W.; software, Z.W.; validation, J.F. and Y.Z.; investigation, Z.W.; resources, S.Z.; data curation, S.Z.; writing—original draft preparation, Z.W.; writing—review and editing, X.L. and Z.W.; visualization, Z.W.; supervision, X.L. and S.Z.; project administration, X.L. All authors have read and agreed to the published version of the manuscript.

Funding: This research was funded by Geochemical evolution of F-bearing diagenetic fluid and dissolution mechanism of siliciclastic particles in tight sandstone, grant number 42172135.

Data Availability Statement: Data will be made available on request.

Acknowledgments: The careful reviews and constructive suggestions of the manuscript by anonymous reviewers are greatly appreciated.

Conflicts of Interest: The authors declare no conflict of interest.

References

1. Zeng, L.B.; Qi, J.F.; Wang, Y.X. Origin type of tectonic fractures and geological conditions in low-permeability reservoirs. *Acta Pet. Sin.* **2007**, *28*, 52–56.
2. Wang, K.; Zhang, R.H.; Dai, J.S.; Wang, J.P.; Zhao, L.B. Fracture characteristics of low permeability sandstone reservoir of Keshen-2 gas field, Kuqa depression. *Pet. Geol. Recovery Effic.* **2016**, *23*, 53–60.
3. Nelson, R.A. *Geologic Analysis of Naturally Fractured Reservoirs*, 2nd ed.; Gulf Professional Publishing: Houston, TX, USA, 2001; pp. 1–81.
4. Fisher, Q.J.; Casey, M.; Harris, S.D.; Knipe, R.J. Fluid-flow properties of faults in sandstone: The importance of temperature history. *Geology* **2003**, *31*, 965–968. [CrossRef]
5. Medici, G.; West, L.J. Review of groundwater flow and contaminant transport modelling approaches for the Sherwood Sandstone aquifer, UK; insights from analogous successions worldwide. *Q. J. Eng. Geol. Hydrogeol.* **2022**, *55*, qjegh2021-176. [CrossRef]
6. Medici, G.; West, L.J. Reply to discussion on 'Review of groundwater flow and contaminant transport modelling approaches for the Sherwood Sandstone aquifer, UK; insights from analogous successions worldwide' by Medici and West (QJEGH, 55, qjegh2021-176). *Q. J. Eng. Geol. Hydrogeol.* **2023**, *56*, qjegh2022-097. [CrossRef]
7. Ding, Z.Y.; Qian, X.L.; Huo, H.; Yang, Y.Q. A new method for quantitative prediction of structural fractures—The binary method. *Oil Gas Geol.* **1998**, *19*, 14.
8. Wu, L.Q.; Liu, C.L.; Zhang, T.; Guo, H.Z.; Xu, J.J.; Jiang, C.Z. The application of "binary method" in quantitative prediction of structural fractures—Taking the shale in the Qingyi section of the Songliao Basin as an example. *J. Geomech.* **2018**, *24*, 598–606.
9. Yu, X.; Hou, G.T.; Li, Y.; Lei, G.L.; Wei, H.X.; Zheng, C.F.; Zhou, L. Quantitative prediction of fractures in the Lower Jurassic Ahe Formation in the three-dimensional exploration area of the Dibei gas field. *Geosci. Front.* **2016**, *23*, 240–252.
10. Zhou, P.; Yin, H.W.; Zhou, L.; Tang, Y.G.; Li, C.S.; Zhu, W.H.; Xie, T.N.; Shang, J.W. Main controlling factors and prediction methods of reservoir in strain middle and plane tension section of faulted anticlinal: A case study of Crassus thrust belt. *Geotecton. et Metallog.* **2018**, *42*, 50–59.
11. Dean, S.L.; Morgan, J.K.; Fournier, T. Geometries of frontal fold and thrust belts: Insights from discrete element simulations Original Research Article. *J. Struct. Geol.* **2013**, *53*, 43–53. [CrossRef]
12. Frehner, M. The neutral lines in buckle folds. *J. Struct. Geol.* **2011**, *33*, 1501–1508. [CrossRef]
13. Zhang, J.; Morgan, J.K.; Gray, G.G.; Harkins, N.W.; Sanz, P.F.; Chikichev, I. Comparative FEM and DEM mode ling of basement-involved thrust structures, with application to Sheep Mountain, Greybull area, Wyoming. *Tectono Phys.* **2013**, *608*, 408–417. [CrossRef]
14. Zhao, L.B.; Dai, J.S.; Sun, Y.; Feng, Z.D.; Xiao, X.J.; Li, Z.Y.; Zhang, J. Application of fractal geometry method to fracture prediction in Kela 2 gas field. *Xinjiang Pet. Geol.* **2012**, *33*, 595–598.
15. Gong, L.; Zeng, L.B.; Miao, F.B.; Wang, Z.S.; Wei, Y.; Li, M.; Zu, K.W. Application of fractal geometry method in the description of complex fracture system. *J. Hunan Univ. Sci. Technol. (Nat. Sci. Ed.)* **2012**, *27*, 6–10.
16. Wang, G.C.; Zhang, C.G.; Tang, J.; Zhu, L.; Ju, D.H.; Cao, J.N. Application of fractional dimension in identifying fractures in deep tight sandstone. *J. Yangtze Univ. (Nat. Sci. Ed.)* **2015**, *12*, 33–36.
17. Wang, C.G.; Lin, X.M.; Zhou, X.H.; Wang, L.; Shen, J.S.; Su, C.Y. Fault detection and evaluation based on fusion of multiple seismic attributes—An example of fractured and vuggy carbonate formation in SHB Area, Tarimu basin. *CT Theory Appl.* **2021**, *30*, 35–48.
18. Rao, S.; Sun, F.T.; Wang, H.Q.; Du, S.G.; Li, C.P. Seismic fracture prediction method based on azimuthal anisotropy theory and its application. *China Energy Environ. Prot.* **2021**, *43*, 152–156.
19. Liu, J.Z.; Han, L.; Shi, L.; Chen, S.Q. Seismic prediction of tight sandstone reservoir fractures in XC area, western Sichuan Basin. *Oil Gas Geol.* **2021**, *42*, 747–754.
20. Wang, K.; Dai, J.S.; Wang, J.P.; Tian, F.C.; Zhao, L.B.; Huan, Z.P. Quantitative prediction of reservoir structural fractures in Keshen 2 Gas field, Tarim Basin. *Geotecton. et Metallog.* **2016**, *40*, 1123–1135.
21. Wang, K.; Zhang, H.; Zhang, R.; Wang, J.; Dai, J.; Yang, X. Characteristics and influencing factors of ultra-deep tight sandstone reservoir structural fracture:a case study of Keshen-2 gas field, Tarim Basin. *Oil Gas Geol.* **2016**, *37*, 715–727+742.
22. Nelson, R.A. *Geologic Analysis of Naturally Fractured Reservoirs*; Gulf Publishing Company: Houston, TX, USA, 1985.
23. Gale, J.F.W.; Laubach, S.E.; Olson, J.E.; Eichhubl, P.; Fall, A. Natural fractures in shale: A review and new observations. *AAPG Bull.* **2014**, *98*, 2165–2216. [CrossRef]
24. Yuan, B.; Dong, X.M.; Guan, X.T.; Zhou, T.Q.; Wang, X. Analysis of Characteristics of Tight Sandstone Reservoir with Porous-Fissure Dual Medium in Toutunhe Formation of Sikeshu Sag. *Acta Sci. Nat. Univ. Pekin.* **2020**, *56*, 449–459.

25. Li, J.F.; Liu, X.H.; Ye, X.M.; Dang, S.G.; Wang, P.F. Study on fracture characterization of sand—Conglomerate reservoir in LD Oilfield of Bohai Bay Basin. *J. Yangtze Univ. (Nat. Sci. Ed.)* **2021**, *18*, 23–29.
26. Han, Y.W.; Wang, G.W.; Ma, H.F. Influence of Argillaceous Content on Mechanical Properties and Failure Characteristics of Sandstone. *Saf. Coal Mines* **2019**, *50*, 46–49+53.
27. Zeng, L.B.; Zhou, T.W. Distribution regularity of reservoir fractures in Kuqa depression, Tarim Basin. *Nat. Gas Ind.* **2004**, *24*, 23–25.
28. Zhang, R.H.; Yang, H.J.; Zou, W.H.; Zhang, H.L.; Chen, G.; Liu, C. Hydrocarbon accumulation mechanism and distribution of large oil and gas fields in Kuqa foreland area. Petroleum Geology Professional Committee, China Petroleum Society, Beijing Petroleum Society. *Compil. Abstr. 8th China Conf. Pet. Syst. Reserv.* **2015**, 359–361.
29. Zhao, J.L.; Wang, J.P.; Liu, C.; Zeng, Q.L.; Dai, J.S. Reservoir Fracture Numerical Simulation of Keshen-2 Blockin Tarim Basin. *Geoscience* **2014**, *28*, 1275–1283.
30. Zhang, R.H.; Wang, J.P.; Ma, Y.J.; Chen, G.; Zeng, Q.L.; Zhou, C.G. The sedimentary microfacies, Palaeogeomorphology and their controls on gas accumulation of deep—Buried cretaceous in Kuqa Depression, Tarim Basin. *J. Geosci.* **2015**, *26*, 667–678. [CrossRef]
31. Feng, J.R.; Gao, J.Y.; Cui, J.G.; Zhou, C.M. The exploration status and research advances of deep and ultra-deep clastic reservoirs. *Adv. Earth Sci.* **2016**, *31*, 718–736.
32. Zhang, H.L.; Zhang, R.H.; Yang, H.J.; Shou, J.F.; Wang, J.P.; Liu, C.; Chen, G. Characterization, and evaluation of ultra-deep fracture-pore tight sandstone reservoirs: A case study of Cretaceous Bashijiqike Formation in Kelasu tectonic zone in Kuqa foreland basin, Tarim, NW China. *Pet. Explor. Dev.* **2014**, *41*, 158–167. [CrossRef]
33. Xiao, J.X.; Lin, C.S.; Liu, J.Y. Depositional Palaeogeography of Cretaceous of Kuqa Depression in Northern Tarim Basin. *Geoscience* **2005**, *19*, 253–260.
34. Wang, J.H.; Wang, H.; Chen, H.H.; Zhao, Z.X.; Liao, Y.T. Research on the tectonic evolution of foreland basins and their responses to deposition and stratigraphy—An example from the Lower Cretaceous in Kuqa Depression. *Earth Sci. Front.* **2007**, *14*, 114–122.
35. Du, J.H.; Wang, Z.M.; Hu, S.Y.; Wang, Q.H.; Xie, H.W. Formation, and geological characteristics of deep giant gas provinces in the Kuqa foreland thrust belt, Tarim Basin, NW China. *Pet. Explor. Dev.* **2012**, *39*, 385–393. [CrossRef]
36. Zhang, Z.Y.; Lin, C.S.; Liu, Y.F.; Liu, J.Y.; Zhao, H.T.; Li, H.; Sun, Q.; Xia, H.; Ma, M.; Liang, Y. Lacustrine to fluvial depositional systems: The depositional evolution of an intracontinental depression and controlling factors, Lower Cretaceous, Northern Tarim Basin, Northwest China. *Mar. Pet. Geol.* **2021**, *126*, 104904. [CrossRef]
37. Wang, K.; Yang, H.J.; Li, Y.; Zhang, R.H.; Ma, Y.J.; Wang, B.; Yu, C.F.; Yang, Z.; Tang, Y.G. Geological characteristics and exploration potential of the northern tectonic belt of Kuqa depression in Tarim Basin. *Acta Pet. Sin.* **2021**, *42*, 885–905.
38. Zhang, R.H.; Wang, K.; Zeng, Q.L.; Yu, C.F.; Wang, J.P. Effectiveness, and petroleum geological significance of tectonic fractures in the ultra-deep zone of the Kuqa foreland thrust belt: A case study of the Cretaceous Bashijiqike Formation in the Keshen gas field. *Pet. Sci.* **2021**, *18*, 728–741. [CrossRef]
39. Wang, K.; Zhang, R.H.; Wang, J.P.; Sun, X.W.; Yang, X.J. Distribution, and origin of tectonic fractures in ultra-deep tight sandstone reservoirs: A case study of Keshen gas field, Kuqa foreland thrust belt, Tarim Basin. *Oil Gas Geol.* **2021**, *42*, 338–353.
40. Yang, H.J.; Li, Y.; Tang, Y.G.; Lei, G.L.; Zhou, P.; Zhou, L.; Xu, A.M.; Xun, Z.P.; Zhu, W.H.; Chen, W.L.; et al. Accumulation conditions, key exploration, and development technologies for Keshen gas field in Tarim Basin. *Acta Pet. Sin.* **2021**, *42*, 399–414. [CrossRef]
41. Chang, B.H.; Tang, Y.L.; Zhu, S.B.; Li, S.L.; Cao, W. Well test characteristics and understandings of the ultra-deep fractured tight sandstone gas reservoirs: A case study on Keshen Gas Field in Tarim Basin. *Pet. Geol. Oilfield Dev. Daqing* **2021**, *40*, 167–174.
42. Fu, X.T.; Wang, Y.M.; Shao, J.B.; Zhu, S.B.; Wang, Y.; Nie, Y.B.; Duan, Q.Q. Characteristics and Effect on Productivity of the Sandstone and Fractures in Ultra-deep and Fractured Tight Sandstone Gas Reservoirs: A Case Study of KS2 Gasfield in Kuqa Depression, Tarim Basin. *Geoscience* **2021**, *35*, 326–337.
43. Zeng, Q.L.; Mo, T.; Zhao, J.L.; Tang, Y.L.; Zhang, R.H.; Xia, J.F.; Hu, C.L.; Shi, L.L. Characteristics, genetic mechanism, and oil & gas exploration significance of high-quality sandstone reservoirs deeper than 7000 m: A case study of the Bashijiqike Formation of Lower Cretaceous in the Kuqa Depression, NW China. *Nat. Gas Ind. B* **2020**, *7*, 38–47.
44. *Geologic Analysis of Naturally Fractured Reservoirs*; Elsevier Inc.: Amsterdam, The Netherlands, 2001.
45. Laubach, S.E.; Olson, J.E.; Gross, M.R. Mechanical and fracture stratigraphy. *AAPG Bull.* **2009**, *93*, 1413–1426. [CrossRef]